Available online at www.sciencedirect.com
SCIENCE DIRECT
Journal of Sound and Vibration 283 (2005) 217–241
JOURNAL OF SOUND AND VIBRATION
www.elsevier.com/locate/jsvi

Multidisciplinary design optimization of mechatronic vehicles with active suspensions

Yuping He, John McPhee*

Mechanical Engineering and Systems Design Engineering, University of Waterloo, Ontario, Canada N2L 3G1

Received 5 September 2003; accepted 10 April 2004

Abstract

A multidisciplinary optimization method is applied to the design of mechatronic vehicles with active suspensions. The method is implemented in a GA-A'GEM-MATLAB simulation environment in such a way that the linear mechanical vehicle model is designed in a multibody dynamics software package, i.e. A'GEM, the controllers and estimators are constructed using linear quadratic Gaussian (LQG) method, and Kalman filter algorithm in Matlab, then the combined mechanical and control model is optimized simultaneously using a genetic algorithm (GA). The design variables include passive parameters and control parameters. In the numerical optimizations, both random and deterministic road inputs and both perfect measurement of full state variables and estimated limited state variables are considered. Optimization results show that the active suspension systems based on the multidisciplinary optimization method have better overall performance than those derived using conventional design methods with the LQG algorithm.

1. Introduction

Conventionally, active elements of vehicle suspensions are designed independently of the passive components [1]. Applied to a vehicle model, such controllers may behave less optimally overall due to not considering the mechanical parameters, e.g. inertial and geometric parameters,

*Corresponding author. Tel.: +1-519-885-1211; fax: +1-519-746-4791.
E-mail addresses: yuping@real.uwaterloo.ca (Y. He), mcphee@real.uwaterloo.ca (J. McPhee).

0022-460X/$ - see front matter
doi:10.1016/j.jsv.2004.04.027

as variables in the design process. An integrated mechanical and control design process may help to achieve an optimal behavior of the overall vehicle. In recent years, several researchers have tackled the task by taking passive parameters and active parameters as design variables simultaneously when designing ground vehicles with active suspensions [1–4].

However, all these researchers have limited their control strategies to the use of ''skyhook'' dampers [5] in their design optimizations. Since the 1970s, the linear quadratic Gaussian (LQG) optimal control method [6] has been widely used in designing controllers for active suspensions. It was shown that the LQG provides a compact analytical solution with relatively low design and computational time, and the stability of the system designed is guaranteed. Moreover, the result of an optimization process is a controller that considers and feeds back all system states with constant gains, while any classical controller structure may not be ensured to be optimal. Although the passive spring stiffness and damping coefficients have been optimized with the control parameters using the LQG algorithm [6], it seems that the vehicle inertial and geometric parameters and control parameters have not been considered as design variables simultaneously in the optimization process using the LQG.

Furthermore, one difficulty in using the LQG is how to determine the weighting factors of the performance index. Traditionally, a 'trial and error' method is used for choosing the weighting factors or the combinations of the factors [6]. To some extent, the optimal design of controllers depends on the experience of designers. For complex design systems and for multicriteria optimization problems in particular, the choice of the weighting factors is a nontrivial problem [7].

Results have shown that combined with multibody dynamics softwares, e.g. A'GEM [8], a genetic algorithm (GA) is an effective approach to the design of rail vehicles with passive and active suspensions [4]. The GA is well-suited to the optimization of complex ground vehicle models now available from multibody simulation programs such as A'GEM, especially when more than a few design variables are being considered.

In general, the design optimization of aircrafts and road vehicles is multidisciplinary [9] and the task is to find effective trade-off solutions for complicated and conflicting design criteria [10]. For example, the simultaneous design of a structure and a control system for the purpose of active flutter suppression for an aircraft is a typical application of multidisciplinary optimization (MDO) [11]. In the case concerned, there are interactions among the wing structure, the control system, and aerodynamics. These interactions make the structure, the control system, and aerodynamics a synergistic whole. Taking advantage of that synergy is the mark of a good design [9]. In fact, multidisciplinary optimization is presently of increasing interest in engineering. MDO received recognition in the aeronautical sciences, first for the structural optimization and later for the aerodynamic design [11]. Currently, we can find the application of MDO to automotive vehicle design for safety and NVH (noise, vibration and harshness) reduction [9,12,13].

The purpose of this study is to extend the work reported in Ref. [4] by using a MDO method, the All-in-One (A-i-O) method [9], for the design of mechatronic vehicles with active suspensions. To demonstrate the efficacy of the MDO method using the GA, A'GEM, LQG, and Kalman filters, the method is used to resolve the conflicting requirements for ride comfort, suspension working spaces, and dynamic wheel loads in the optimization of quarter-vehicle models with active suspensions. Both deterministic and random road excitations, and both perfect measurement of full state variables and estimated limited state variables are considered. The A-i-O method is implemented in a GA-A'GEM-MATLAB simulation environment in such a way that the linear mechanical vehicle model is generated in A'GEM, the controllers and Kalman filters are modelled in MATLAB, then the combined mechanical and control model is optimized simultaneously using the GA.

In the following sections, first, the LQG and Kalman filter algorithms are recalled briefly; second, the vehicle models are introduced; third, the A-i-O method and its implementation are described; finally, the numerical simulation results for linear quarter-vehicle models are presented.

2. LQG and Kalman filer algorithms

In this section, the LQG control algorithm [6,7,15–17] is outlined, then the Kalman filter algorithm [7,16,17] is recalled. The "separation principle" [7] was adopted in the development of the LQG controller and Kalman estimator. First, the optimal controller is designed as if full state feedback is available. Second, the optimal estimator is designed to provide the full state estimation.

2.1. LQG control strategy

The LQG control strategy can be described as an optimization problem: minimize the objective function or performance index

$$J = \lim_{T\to\infty} \frac{1}{T} E\left\{ \int_0^T \begin{bmatrix} \mathbf{x}_a \\ \mathbf{u} \end{bmatrix}^T \begin{bmatrix} \mathbf{G} & \mathbf{N} \\ \mathbf{N}^T & \mathbf{H} \end{bmatrix} \begin{bmatrix} \mathbf{x}_a \\ \mathbf{u} \end{bmatrix} \mathrm{d}t \right\} \tag{1}$$

subject to

$$\dot{\mathbf{x}}_a = \mathbf{A}_a\mathbf{x}_a + \mathbf{B}_a\mathbf{u} + \mathbf{D}_a\boldsymbol{\xi}, \tag{2}$$

where $\mathbf{x}_a$ is the state variable vector including system states and input states, $\mathbf{u}$ is the actuator force vector, and $\boldsymbol{\xi}$ is the disturbance vector assumed to be white-noise processes with zero mean and covariance matrix $\mathbf{Q}$. $\mathbf{G}$, $\mathbf{N}$, and $\mathbf{H}$ are weighting matrices. $\mathbf{A}_a$, $\mathbf{B}_a$, and $\mathbf{D}_a$ are the system, control, and disturbance matrices, respectively. For the linear time-invariant system, $\mathbf{A}_a$, $\mathbf{B}_a$, $\mathbf{D}_a$, $\mathbf{G}$, $\mathbf{N}$, and $\mathbf{H}$ are all constant matrices with proper dimensions.

It is assumed that all uncontrollable modes are stable. Thus, the solution of the optimization problem is the control force vector of the form

$$\mathbf{u} = -\mathbf{K}\mathbf{x}_a, \tag{3}$$

where $\mathbf{K}$ is the control gain matrix with the dimension of $m \times n$. An arbitrary entry, K_{ij}, is determined by the solution of

$$\frac{\partial J}{\partial K_{ij}} = 0, \tag{4}$$

From Eq. (4), the gain matrix $\mathbf{K}$ can be obtained as

$$\mathbf{K} = \mathbf{H}^{-1}(\mathbf{N}^T + \mathbf{B}_a^T\mathbf{S}), \tag{5}$$

where the symmetric and positive-definite matrix $\mathbf{S}$ is a solution of the Riccati equation

$$\mathbf{S}\mathbf{A}_a + \mathbf{A}_a^{\mathrm{T}}\mathbf{S} + \mathbf{G} - (\mathbf{S}\mathbf{B}_a + \mathbf{N})\mathbf{H}^{-1}(\mathbf{S}\mathbf{B}_a + \mathbf{N})^{\mathrm{T}} = \mathbf{0}. \tag{6}$$

The covariance matrix $\mathbf{X}_a$ of the state variable vector $\mathbf{x}_a$ is defined as

$$\mathbf{X}_a = E[\mathbf{x}_a\mathbf{x}_a^{\mathrm{T}}], \tag{7}$$

where E denotes the expected value. The matrix $\mathbf{X}_a$ is determined by the Lyapunov equation

$$(\mathbf{A}_a - \mathbf{B}_a\mathbf{K})\mathbf{X}_a + \mathbf{X}_a(\mathbf{A}_a - \mathbf{B}_a\mathbf{K})^{\mathrm{T}} + \mathbf{D}_a\mathbf{Q}\mathbf{D}_a^{\mathrm{T}} = \mathbf{0}. \tag{8}$$

The resulting performance index is

$$J_{\mathrm{opt}} = \mathrm{trace}(\mathbf{S}\mathbf{D}_a\mathbf{Q}\mathbf{D}_a^{\mathrm{T}}). \tag{9}$$

It should be noted that if the state vector $\mathbf{x}_a$ includes input states, the system considered is not completely controllable. This is because the road input can not be changed by applying a control force. In this case, the Riccati equation (6) and the Lyapunov equation (8) can still be solved numerically after partitioning the corresponding unknown matrix $\mathbf{S}$ and state covariance matrix $\mathbf{X}_a$ into four submatrices. This method has been offered in detail by Hac [15].

It is worth mentioning that for the LQG control strategy, the disturbance vector $\boldsymbol{\xi}$ should be a pure white-noise process. However, in ride quality analysis for vehicles, the road profiles are often modelled as displacement spectral density functions with the characteristics of filtered white noise or integrated white noise [17]. In the first case, the filtered white noise (road input) can be generated from the pure white-noise process $\boldsymbol{\xi}$ using a shaping filter with the form of a first-order differential equation. Thus, if the road input is treated as an additional state variable, the LQG is applicable to the ride quality analysis. This is the random road input case that will be discussed in Sections 3.2 and 6.2. In the integrated white-noise road input case, for a linear vehicle system, the mean-squared value of any output signal of interest is simply related to the integral-squared value of the corresponding output signal due to a unit step input. For a given velocity, if the system is optimal for a unit step input, it will also be optimal for the corresponding integrated white-noise road input [6]. With this equivalence and the appropriate selection of state variables, the LQG problem is reduced to an equivalent linear quadratic regulator (LQR) problem. This is the deterministic road input case that will be discussed in Sections 3.1 and 6.1. For other kinds of road inputs, such as a pothole, provided that the integral of the squared value of an output signal of interest due to the input converges, as in the case of a unit step road input, the corresponding LQR problem may be solved. However, the controller designed is not guaranteed to be optimal for regular random road conditions.

2.2. *Kalman filter algorithm*

The LQG outlined in the previous subsection assumes perfect measurement of all the state variables. In practice, not all the state variables are available but only a limited number of the states. In addition, the corresponding measurements are noisy, which further degrades the performance of the control systems.

It is assumed that the measurements are corrupted by noise and the measurement equation can be formulated as

$$\mathbf{y}_a = \mathbf{C}_a\mathbf{x}_a + \boldsymbol{\upsilon}, \tag{10}$$

where $\mathbf{y}_a$ is the output vector, $\mathbf{C}_a$ is the output matrix or the state-to-measurement transformation matrix, and $\mathbf{x}_a$ is the state variable vector including system states and input states. $\boldsymbol{\upsilon}$ is assumed to be Gaussian white-noise process vector with zero mean and covariance matrix $\mathbf{R}$ described by

$$E[\boldsymbol{\upsilon}(t)] = \mathbf{0}, \quad E[\boldsymbol{\upsilon}(t)\boldsymbol{\upsilon}^{\mathrm{T}}(\tau)] = \mathbf{R}\delta(t-\tau), \tag{11}$$

where $\mathbf{R}$ is a positive-definite matrix with proper dimension.

Thus, the optimal estimator can be formulated as

$$\dot{\hat{\mathbf{x}}}_a = \mathbf{A}_a\hat{\mathbf{x}}_a + \mathbf{B}_a\mathbf{u} + \mathbf{L}(\mathbf{y}_a - \mathbf{C}_a\hat{\mathbf{x}}_a), \tag{12}$$

where $\hat{\mathbf{x}}_a$ is the optimal estimate vector of the state variable vector $\mathbf{x}_a$, $\mathbf{u}$ is the actuator force vector, $\mathbf{A}_a$ and $\mathbf{B}_a$ are augmented system and control matrices defined previously, and $\mathbf{L}$ is the Kalman filter gain matrix that is determined by

$$\mathbf{L} = \mathbf{P}\mathbf{C}_a^{\mathrm{T}}\mathbf{R}^{-1}, \tag{13}$$

where $\mathbf{P}$ is the filter error ($\mathbf{e} = \hat{\mathbf{x}}_a - \mathbf{x}_a$) covariance matrix which can be found from the following steady-state matrix Riccati equation:

$$\mathbf{A}_a\mathbf{P} + \mathbf{P}\mathbf{A}_a^{\mathrm{T}} + \mathbf{Q}_1 - \mathbf{P}\mathbf{C}_a^{\mathrm{T}}\mathbf{R}^{-1}\mathbf{C}_a\mathbf{P} = \mathbf{0}. \tag{14}$$

Notice that for the quarter-vehicle models used in the research, the systems $(\mathbf{A}_a, \mathbf{C}_a)$ are observable. Thus, unlike the cases for solving Eqs. (6) and (8), the Riccati equation denoted by Eq. (14) can be solved directly without partitioning the unknown matrix $\mathbf{P}$ and relevant matrices into four submatrices and then solving the corresponding equations.

3. Vehicle system models

Fig. 1 shows the quarter-vehicle model to be optimized. Two different cases, i.e. deterministic and stochastic road inputs, are considered.

3.1. Deterministic road input case

To compare the simulation results from the A-i-O method with published results, the vehicle model is based on that used by Thompson [6]. As shown in Table 1, the nominal vehicle parameters are listed as Set 1. It should be noted that to determine the control force $\mathbf{u}$ using the LQG, in Thompson's vehicle model, $k_2 = 0$, $c_2 = 0$, and other passive vehicle system parameters take their nominal values. Moreover, in a "physical realization" of the control force $\mathbf{u}$, Thompson divided the force determined by the LQG into two sections, i.e. passive spring and damper force and actuator force. However, in our study, for simplicity, the control force $\mathbf{u}$, determined by the LQG, is defined as actuator force.

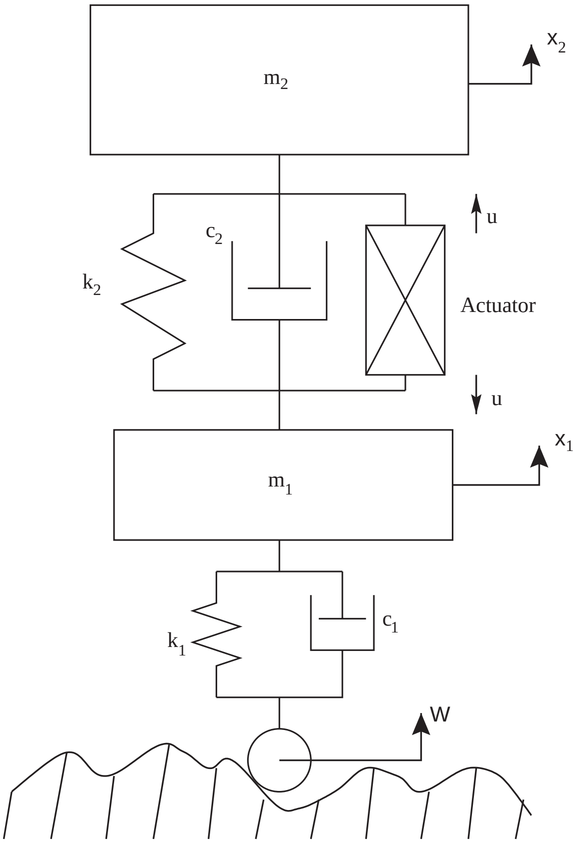

Fig. 1. 2 DOF quarter-vehicle models.

Table 1
Nominal vehicle parameters and road characteristic parameters

	m_1 (kg)	m_2 (kg)	k_1 (N/m)	c_1 (N/m/s)	k_2 (N/m)	c_2 (N/m/s)	a_t (1/m)	σ_t (1/m^2)
Set 1	28.58	288.9	1.559×10^5	0.0	1.996×10^4	1.861×10^3		
Set 2	100.0	500.0	2.0×10^5	0.0	5.0×10^3	1.0×10^3	0.45	9.0×10^{-6}

The road input vector is represented by **w** with dimension of 1×1. The actuator force vector **u**, with dimension of 1×1, is applied equally to the sprung mass (m_2) and the unsprung mass (m_1).

The state variable vector **x** is assumed to take the form

$$\mathbf{x} = \begin{bmatrix} x_1 - w & x_2 - w & \dot{x}_1 & \dot{x}_2 \end{bmatrix}^{\mathrm{T}}, \tag{15}$$

where w is the scalar expression of the vector **w**. Thus, the governing equations of motion of the 2 DOF model can be written in state space form as

$$\dot{\mathbf{x}} = \mathbf{A}\mathbf{x} + \mathbf{B}\mathbf{u} + \mathbf{D}\dot{\mathbf{w}}, \quad \mathbf{y} = \mathbf{C}\mathbf{x}, \tag{16}$$

where **u** is the actuator force vector of dimension 1×1, $\dot{\mathbf{w}}$ is the road velocity excitation vector of dimension 1×1, **y** is the output vector of dimension 2×1, **A**, **B**, **C**, and **D** are the system matrix, control matrix, output matrix, and disturbance matrix, respectively, which are

$$\mathbf{A} = \begin{bmatrix} 0 & 0 & 1 & 0 \\ 0 & 0 & 0 & 1 \\ -\dfrac{k_1+k_2}{m_1} & \dfrac{k_2}{m_1} & -\dfrac{c_1+c_2}{m_1} & \dfrac{c_2}{m_1} \\ \dfrac{k_2}{m_2} & -\dfrac{k_2}{m_2} & \dfrac{c_2}{m_2} & -\dfrac{c_2}{m_2} \end{bmatrix}, \quad \mathbf{B} = \begin{bmatrix} 0 & 0 & -\dfrac{1}{m_1} & \dfrac{1}{m_2} \end{bmatrix}^{\mathrm{T}},$$

$$\mathbf{C} = \begin{bmatrix} 1 & 0 & 0 & 0 \\ 0 & 1 & 0 & 0 \end{bmatrix}, \quad \mathbf{D} = \begin{bmatrix} -1 & -1 & \dfrac{c_1}{m_1} & 0 \end{bmatrix}^{\mathrm{T}}. \tag{17}$$

Note that the relative distance, e.g. $x_2 - w$ or $x_1 - w$, may be measured by the acoustic (or radar) transmitter and receiver system proposed by Thompson [6,22]. The absolute sprung mass and unsprung mass vertical velocities, i.e. $\dot{x}_2$ and $\dot{x}_1$, may be obtained from the integrated output of accelerometers mounted on the sprung mass and unsprung mass, respectively.

3.2. Random road input case

In the random road input case, the vehicle model used, as shown in Fig. 1, is based on that used by Hac [15]. Notice that to determine the actuator force **u**, in Hac's vehicle model, the parameters including k_2 and c_2 take their nominal values listed in Table 1 as Set 2.

The road input **w** is a filtered white-noise process. The power spectral density (PSD) of the filtered white-noise road displacement excitation can be formulated as [15,20,21]

$$S_w(\omega) = (\sigma_t/\pi)a_t V/(\omega^2 + a_t^2 V^2), \tag{18}$$

where σ_t is the variance of road irregularities and a_t is the road roughness constant. The process **w** (with dimension of 1×1) with the PSD (expressed in (18)) can be generated from the pure white-noise process $\boldsymbol{\xi}$ (with dimension of 1×1) using a shaping filter of the form

$$\dot{\mathbf{w}} = -a_t V \mathbf{w} + \boldsymbol{\xi}. \tag{19}$$

In this case, the state variable vector **x** is expressed as

$$\mathbf{x} = \begin{bmatrix} x_1 & x_2 & \dot{x}_1 & \dot{x}_2 \end{bmatrix}^{\mathrm{T}}. \tag{20}$$

Then the governing equations of the 2 DOF vehicle model can be written as

$$\dot{\mathbf{x}} = \mathbf{A}\mathbf{x} + \mathbf{B}\mathbf{u} + \mathbf{D}_1\mathbf{w} + \mathbf{D}_2\dot{\mathbf{w}}, \tag{21}$$

where $\mathbf{u}$ is the actuator force vector with dimension of 1×1. The matrices $\mathbf{A}$ and $\mathbf{B}$ are the same as those offered in equation set (17). The matrices $\mathbf{D}_1$ and $\mathbf{D}_2$ take the forms

$$\mathbf{D}_1 = \begin{bmatrix} 0 & 0 & \frac{k_1}{m_1} & 0 \end{bmatrix}^{\mathrm{T}}, \quad \mathbf{D}_2 = \begin{bmatrix} 0 & 0 & \frac{c_1}{m_1} & 0 \end{bmatrix}^{\mathrm{T}}. \tag{22}$$

If the augmented state vector $\mathbf{x}_a$ takes the form

$$\mathbf{x}_a = \begin{bmatrix} \mathbf{x}^{\mathrm{T}} & \mathbf{w}^{\mathrm{T}} \end{bmatrix}^{\mathrm{T}} \tag{23}$$

then based on Eqs. (19), (20), (23), and (21), we have the augmented state space equations

$$\dot{\mathbf{x}}_a = \mathbf{A}_a\mathbf{x}_a + \mathbf{B}_a\mathbf{u} + \mathbf{D}_a\boldsymbol{\xi}, \quad \mathbf{y}_a = \mathbf{C}_a\mathbf{x}_a, \tag{24}$$

where the matrices $\mathbf{A}_a$, $\mathbf{B}_a$, and $\mathbf{D}_a$ are given as

$$\mathbf{A}_a = \begin{bmatrix} \mathbf{A} & \mathbf{D}_1 + \mathbf{D}_2 \\ \mathbf{0}_{1\times 4} & \mathbf{I}_{1\times 1} \end{bmatrix}, \quad \mathbf{B}_a = \begin{bmatrix} \mathbf{B}^{\mathrm{T}} & \mathbf{0}_{1\times 1} \end{bmatrix}^{\mathrm{T}}, \quad \mathbf{D}_a = \begin{bmatrix} \mathbf{D}_2^{\mathrm{T}} & \mathbf{I}_{1\times 1} \end{bmatrix}^{\mathrm{T}}, \tag{25}$$

where $\mathbf{I}$ denotes identity matrix. Note that if the measurements are corrupted by noise, the second equation of (24) should take the form of Eq. (10) and $\boldsymbol{\upsilon}$ is assumed to be a Gaussian white-noise process with zero mean and covariance matrix $\mathbf{R}$ described by Eq. (11).

It is assumed that either all the state variables are available or just the sprung mass and unsprung mass velocities are available. As in the case of deterministic road input, the absolute sprung mass and unsprung mass vertical velocities may be obtained from the integrated output of accelerometers mounted on the sprung mass and unsprung mass, respectively. Therefore, the output matrix $\mathbf{C}_a$ takes the form of $\mathbf{I}_{5\times 5}$ or

$$\mathbf{C}_a = \begin{bmatrix} 0 & 0 & 1 & 0 & 0 \\ 0 & 0 & 0 & 1 & 0 \end{bmatrix} \tag{26}$$

correspondingly.

4. Combination of vehicle dynamic system, LQG controller, and Kalman estimator

With the vehicle dynamic system described in Eqs. (18) and (24), and the LQG controller and Kalman estimator designed previously based on the separation principle, we can obtain the strongly coupled vehicle dynamic system, controller, and estimator as shown in Fig. 2 using a cascade arrangement.

With the assembled system, the performance index of the optimally controlled system is given by

$$J_{\mathrm{opt}} = \mathrm{trace}(\mathbf{S}\mathbf{D}_a\mathbf{Q}\mathbf{D}_a^{\mathrm{T}}) + \mathrm{trace}(\mathbf{K}^{\mathrm{T}}\mathbf{H}\mathbf{K}\mathbf{P}). \tag{27}$$

The performance index, given by Eq. (27), consists of two parts. The first part results from the random road excitation while the second part is due to the measurement errors. The presence of measurement error increases the performance index since $\mathrm{trace}(\mathbf{K}^{\mathrm{T}}\mathbf{H}\mathbf{K}\mathbf{P})$ is, in general, positive.

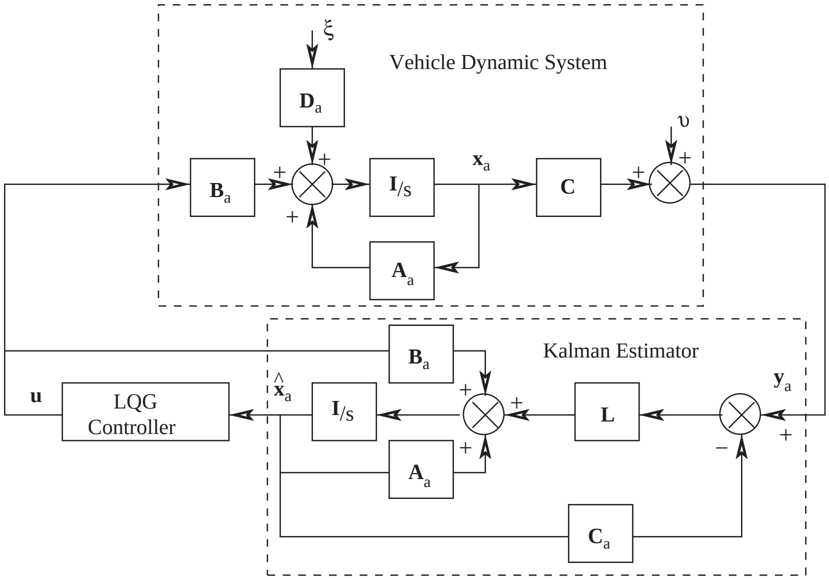

Fig. 2. Cascade arrangement of vehicle dynamic system, Kalman estimator, and LQG controller.

5. Multidisciplinary optimization and implementation

5.1. Design optimization approach

A successful vehicle system design requires harmonization of a number of criteria and constraints [9]. Such a design problem can be modelled as a constrained optimization in the design variable space. However, for such optimization, due to its dimensionality, complexity, and expense for analysis, a decomposition approach is recommended so as to enable concurrent execution of smaller and more manageable tasks [9]. To preserve the couplings that naturally occur among the subsystems of the whole problem, such optimization by various types of decomposition must include a degree of coordination at the system and subsystem levels. MDO offers effective methods for performing the above optimization so as to resolve the trade-off relations among the various design criteria at the system and subsystem levels.

Several MDO methods exist, including the All-in-One (A-i-O) method. The A-i-O method is commonly used for the solution of MDO problems. This method has been offered in detail by Kodiyalam and Sobieski [9]. In our study, the A-i-O method is applied to the vehicle system design for optimizing the mechanical system, controller, and estimator simultaneously. Fig. 3 shows the schematic representation of the design optimization approach.

The system shown in Fig. 3 is composed of an optimizer, i.e. a genetic algorithm, which manipulates the relevant objective function and constraints, and three disciplines, i.e. the vehicle dynamic system with A'GEM software, the optimal estimator with Kalman filter algorithm, and the optimal controller with LQG control algorithm. The A-i-O approach to this optimization problem is a two-level optimization method. The optimization problem is solved for each discipline as well as for the system as a whole. The system is nonhierarchical because each

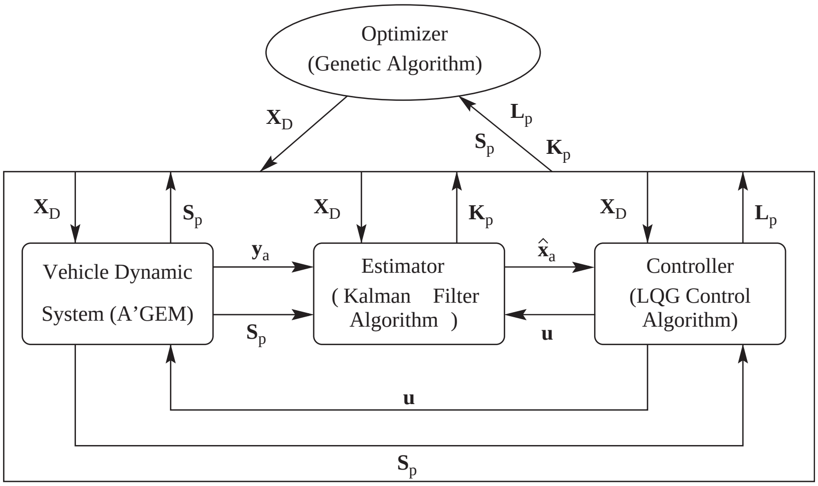

Fig. 3. Schematic representation of the design optimization approach.

discipline is coupled to every other discipline, and no discipline is viewed as being "above" the others.

After a generation of evolution, a potential individual design variable set $\mathbf{X}_D$ is provided by the GA to the coupled analysis disciplines. The design variable set $\mathbf{X}_D$ may include the passive design variables for the vehicle system, e.g. inertial property parameters and passive suspension parameters, and control parameters such as the weighting factors required in Eq. (1). With this set of design variables, a complete system multidisciplinary analysis is performed to obtain vehicle dynamic system output variable vector $\mathbf{y}_a$, optimal estimate vector $\hat{\mathbf{x}}_a$, and actuator force vector $\mathbf{u}$, which are used for evaluating the corresponding subsystem objective functions and constraints. In addition to these coupled variables among the three disciplines, the resulting vehicle system parameters $\mathbf{S}_p$, e.g., the system matrix $\mathbf{A}_a$ generated by A'GEM software, are offered to the Kalman filter algorithm and the LQG control algorithm from the vehicle dynamic system for evaluating the above coupled variables. The vehicle system parameters $\mathbf{S}_p$ together with the resulting Kalman estimator parameters $\mathbf{K}_p$ and the resulting LQG controller parameters $\mathbf{L}_p$ are returned to the optimizer for the evaluation of the system objective function and constraints.

5.2. Implementation of the optimization problem

As shown in Fig. 4, the A-i-O method is implemented using a two-loop optimization approach. In the interior loop, the LQG and Kalman filter algorithms are utilized to optimize the controller and estimator, respectively. In the outer loop, a GA is used to optimize the combined mechanical and control systems.

GAs offer the following advantages over traditional optimization algorithms [14]: (1) higher reliability to find the global optima; (2) finding good designs by manipulating the material of binary strings (corresponding to design variables) without any knowledge of the problem the GA is solving; (3) simple yet powerful in its search for improvement and not limited to the search

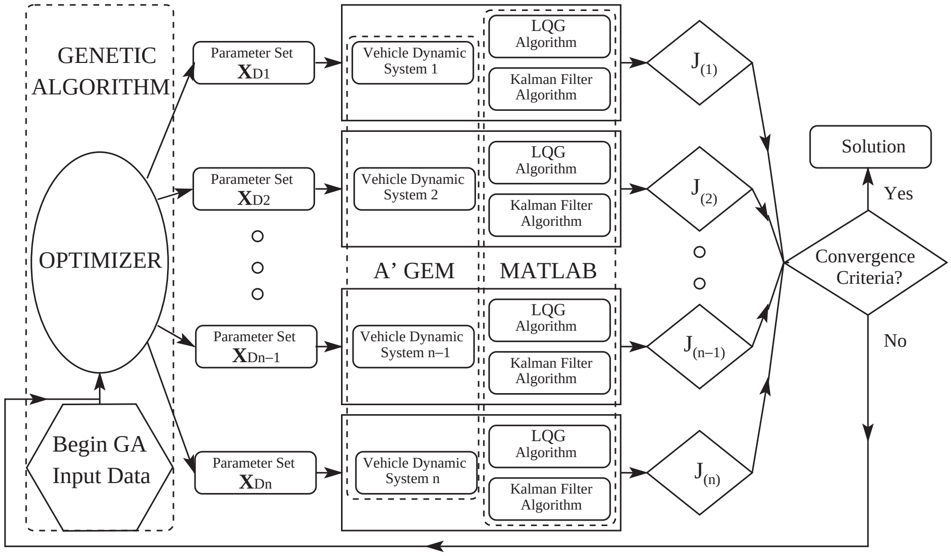

Fig. 4. Schematic representation of the implementation for the All-in-One method.

space, such as continuity or existence of derivatives; (4) guiding its searches using probability rules. A population of designs evolves from generation to generation through the application of genetic operators, such as selection, crossover, and mutation. Selection is a process in which individual strings (designs) are copied based on their fitness values. Highly fit strings have a higher number of offspring in the succeeding generation. Crossover is a method of combining successful designs by exchanging design characteristics among randomly selected pairs from the selected population. A crossover site is selected at random. Mutation is a technique that introduces new information into the new population at the bit level. A set of bits are selected randomly within the entire population.

The GA, called MechaGen program [3] and based on Goldberg's GA [14], was written in C using pseudo-random number generators linked from the NAG (Numerical Algorithm Group) Fortran library. Two techniques were introduced in the program: (1) using a linear search look-up table for the purpose of improving the efficiency of the GA; (2) ranking the population according to fitness values to avoid premature termination of the algorithm.

The LQG and Kalman filter algorithms are used for optimizing the controller and estimator, respectively, provided the mechanical system is given. For a vehicle system with a given set of design parameters $\mathbf{X}_{Di}$, including inertial parameter vector $\mathbf{In}_i$, geometric parameter vector $\mathbf{G}_i$, and passive suspension parameter vector $\mathbf{S}_i$, A'GEM can be used to automatically generate the vehicle system matrix $\mathbf{A}_{ai}$ (see $\mathbf{A}_a$ in Eq. (2)) in a state space form. Here, the index i represents the ith individual design variable set of a population of n in a certain generation.

As illustrated in Fig. 4, first, a population of n sets of design variables, $\mathbf{X}_{Di}, i = 1, 2, \ldots, n$, are randomly selected in the search space by the GA; the corresponding sets of design variables are sent in parallel to the A'GEM routines which automatically generate the governing equations of motion of the vehicle system in a state space form. With the required system matrix $\mathbf{A}_{ai}$ and weighting factors ρ_i, the LQG and Kalman filter algorithms in MATLAB construct and optimize the corresponding controller and estimators resulting in control gain matrix $\mathbf{K}_i$, covariance matrix $\mathbf{X}_{ai}$ of the state variables, filter error covariance matrix $\mathbf{P}_i$, and performance index J_i. Then these performance indices, i.e. $\{J_1, J_2, \ldots, J_n\}^{\mathrm{T}}$, are used as the fitness values. At this point, if the convergence criteria are satisfied, the calculation terminates; otherwise, these fitness values are returned to the GA. Based on the returned fitness values corresponding to the given sets of design variables, the GA produces the next generation of design variables sets using genetic operators, e.g. selection, crossover, and mutation. This procedure repeats until the optimized variable set is found.

In the study, all simulations were carried out on a Silicon Graphics Indigo 2 XZ workstation (circa 1995). The GA (MechaGen program written in C), A'GEM package (written in Fortran), and Matlab (version 5.2) were linked by a main Fortran program and automatically implemented on the workstation. In the numerical experiments of the A-i-O method shown in Fig. 4, it was found by trial and error that the selected GA parameters, a crossover probability of 100%, a mutation probability of 1.0%, and a population size (the number of design variable sets) of 100, give fairly consistent results.

In the deterministic road input case, to optimize the passive vehicle variables (m_1, m_2, k_1, k_2, and c_2) and control gain matrix $\mathbf{K}$, the elapsed time of operating the A-i-O method took 7.78 h for 6603 fitness evaluations. In the random road input case, the operation of the A-i-O method required 3.89 h for 4290 fitness evaluations. It was observed that opening the Matlab engine (once per fitness evaluation) from the main Fortran program occupied a large portion of the elapsed time. Therefore, if the routines for LQG and Kalman filter algorithms are coded in Fortran or C and combined with the main Fortran program (instead of running these routines in Matlab), the A-i-O method will be much more efficient. With the parallelism property of the GA, the A-i-O method is suitable for applications using massively parallel computers. If the current applications are implemented in a massively parallel computer system, the computation time could be reduced approximately by a factor of the population size of the GA.

6. Numerical simulations

In this section, the numerical simulation results are presented and discussed. The simulations are carried out in two different cases, i.e. the road inputs are deterministic and stochastic disturbances. The A-i-O method is used to resolve the conflicting requirements for ride comfort, suspension work spaces, and dynamic wheel loads for road vehicles based on the quarter-vehicle models.

6.1. Deterministic road input case

6.1.1. Vehicle system optimization

The optimization problem can be stated as: minimize the objective function

$$J = \int_0^\infty [\rho_1(u + vf_{\text{pass}})^2 + \rho_2\ddot{x}_2^2 + \rho_3(x_1 - w)^2 + \rho_4(x_2 - x_1)^2]\,\mathrm{d}t \tag{28}$$

Table 2
Expressions represented by symbols J_1, J_2, J_3 and J_4

J_1	J_2	J_3	J_4
$\int_0^\infty (u + v f_{\text{pass}})^2 \,dt$	$\int_0^\infty \ddot{x}_2^2 \,dt$	$\int_0^\infty (x_1 - w)^2 \,dt$	$\int_0^\infty (x_2 - x_1)^2 \,dt$

subject to

$$\dot{\mathbf{x}} = \mathbf{Ax} + \mathbf{Bu} + \mathbf{D}\dot{\mathbf{w}}, \tag{29}$$

where v is a constant, ρ_1, ρ_2, ρ_3, and ρ_4 are weighting factors that impose penalties upon the magnitude and durations of the secondary suspension force including actuator force u and passive suspension force f_{pass}, the ride comfort $\ddot{x}_2$, the tire deflection $x_1 - w$, and the suspension working space $x_2 - x_1$, respectively. The initial state variables $x_1(0)$, $x_2(0)$, $\dot{x}_1(0)$, and $\dot{x}_2(0)$ take the values of zero. The road displacement disturbance w is a unit step input at time $t = 0$. Note that u and w are scalar expressions of 1×1 vectors $\mathbf{u}$ and $\mathbf{w}$, respectively.

For simplicity, Eq. (28) is rewritten as

$$J = \sum_{i=1}^{4} \rho_i J_i, \tag{30}$$

where definitions of the symbols J_1, J_2, J_3 and J_4 are offered in Table 2.

As will be discussed later, to facilitate the optimization and the control law synthesis [16,18,19], each term of the right-hand side of Eq. (28) is normalized with the corresponding norm. In the case concerned, the norm of each term is the inverse of the corresponding weighting factor. The weighting factors are assumed to be

$$\rho_i = 1/J_i^{\text{ref}}, \tag{31}$$

where $i = 1, 2, 3, 4$, and J_i^{ref} is the ith term of the objective function (in the form of Eq. (28)) of a reference quarter-vehicle model with passive or active suspensions. Note that the definition of J_i^{ref} ($i = 1, 2, 3, 4$) is the same as its counterpart (J_i) shown in Table 2.

To find the solution to the optimization problem, Eq. (28) should be rewritten in the standard form as shown in Eq. (1). Note that in the deterministic road input case, the input is not treated as an independent state variable as in the case of random road input.

The problem is actually an optimal tracking problem with the addition of a road disturbance $\dot{\mathbf{w}}$. Then the tracking problem is reduced to an equivalent regulator problem. Moreover, for the deterministic road input case, the Kalman estimator is not introduced.

6.1.2. Results and discussion

In this subsection, the simulation results from the A-i-O method are discussed and compared with those provided by Thompson [6]. As will be seen, the optimized vehicle model based on the A-i-O has better performance than the corresponding model with passive suspension and that based on the LQG algorithm (used by Thompson) in all four aspects: ride comfort, suspension working space, dynamic wheel load, and actuator force. Note that the simulation results reported by Thompson [6] have been accurately repeated in this research.

It should be mentioned that in Thompson's numerical simulation [6], the step input of ground position was set as 1 [m], which is too large, yielding a peak acceleration of the sprung mass of about 25 g, excessive tire and suspension deflections, and excessive tire and suspension forces. Under these conditions, the linear vehicle model is not valid. With this consideration, in the current study, the step input of ground position is set as 0.01 [m]; the resulting responses for the linear model scale down accordingly, giving moderate deflections and forces.

When the quarter-vehicle model with active suspension offered by Thompson [6] is selected as a reference vehicle model, the weighting factors ρ_1, ρ_2, ρ_3, and ρ_4 are calculated to take the values of 0, 6.493×10^{-4}, 74.709, and 13.206, respectively. By including m_1, m_2, k_1, k_2, and c_2 as additional design variables, the control gain matrix **K** obtained using the A-i-O and that offered by Thompson using the LQG are listed in Table 3. These additional passive design variables are permitted to vary by 20% from the nominal values. The optimized passive design variables based on the A-i-O, together with their nominal values (listed in Table 1 as Set 1), are provided in Table 4.

The resulting unit step responses based on the A-i-O, the LQG (used by Thompson), and the corresponding passive suspension system are shown in Figs. 5–8. Note that in the case of passive suspension system shown in Figs. 5–8, the vehicle system parameters (m_1, m_2, k_1, c_1, k_2, and c_2)

Table 3
Feedback control gain matrix for optimal suspensions

	$K_{1,1}$	$K_{1,2}$	$K_{1,3}$	$K_{1,4}$
LQG[a]	−57240.0	35355.0	−1385.7	4827.0
A-i-O[b]	−48683.0	26607.0	240.0	4682.0
A-i-O1[c]	−15045.0	11265.0	886.0	2873.0

[a]Thompson's results with passive design variables taking nominal values.
[b]Obtained using the A-i-O with $\rho_1 = 0$.
[c]Obtained using the A-i-O with $\rho_1 = 7.7793 \times 10^{-9}$.

Table 4
Optimal values for m_1, m_2, k_1, k_2, and c_2

	m_1 (kg)	m_2 (kg)	k_1 (N/m)	k_2 (N/m)	c_2 (N/m/s)
NV[a]	28.58	288.9	1.5590×10^5	1.9960×10^4	1.8610×10^3
A-i-O[b] (±20%)	22.864	346.68	1.2472×10^5	2.2836×10^4	1.6698×10^3
A-i-O1[c] (±20%)	22.864	346.68	1.2472×10^5	2.0388×10^4	1.8821×10^3

[a]Nominal values.
[b]Optimized values based on the A-i-O with $\rho_1 = 0$.
[c]Optimized values based on the A-i-O with $\rho_1 = 7.7793 \times 10^{-9}$.

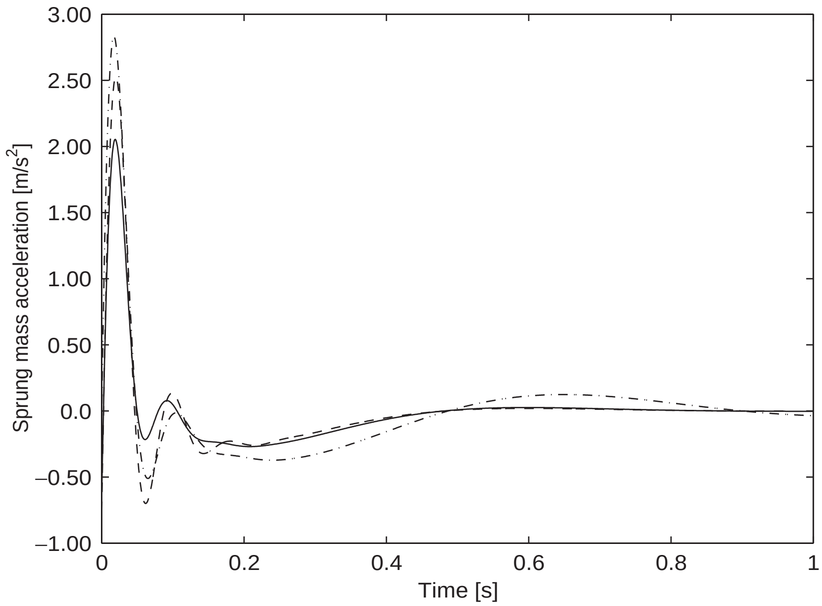

Fig. 5. Sprung mass acceleration versus time: · – ··, passive; – –, LQG; —, A-i-O.

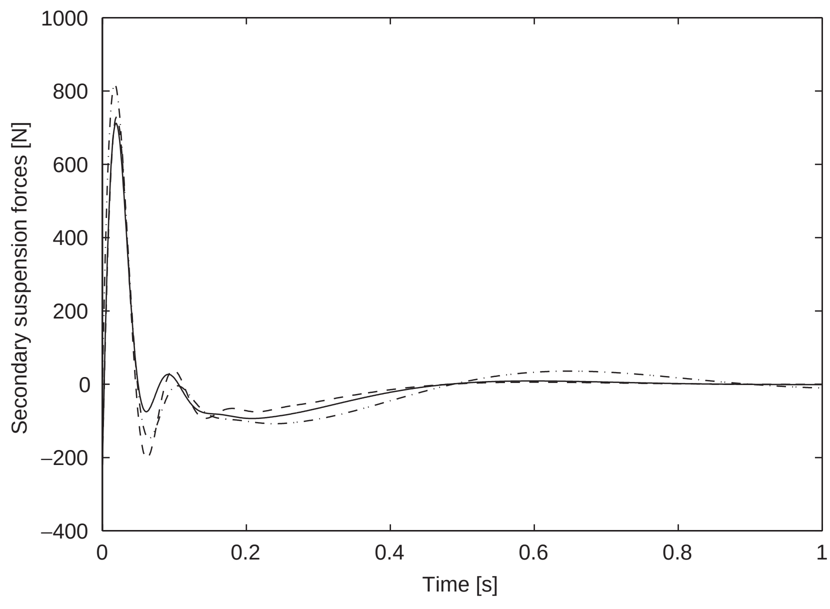

Fig. 6. Secondary suspension forces versus time: · – ··, passive; – –, LQG; —, A-i-O.

take their nominal values listed in Table 1 as Set 1. Fig. 5 illustrates the relationship between the sprung mass acceleration and time, Fig. 6 the secondary suspension forces and time, Fig. 7 the sprung mass displacement and time, and Fig. 8 the unsprung mass displacement and time.

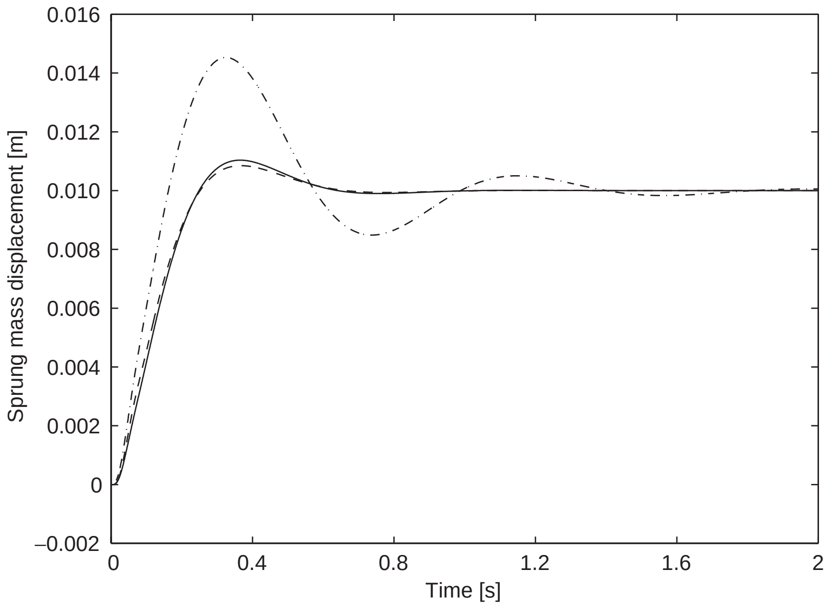

Fig. 7. Sprung mass displacement versus time: · – ··, passive; – –, LQG; —, A-i-O.

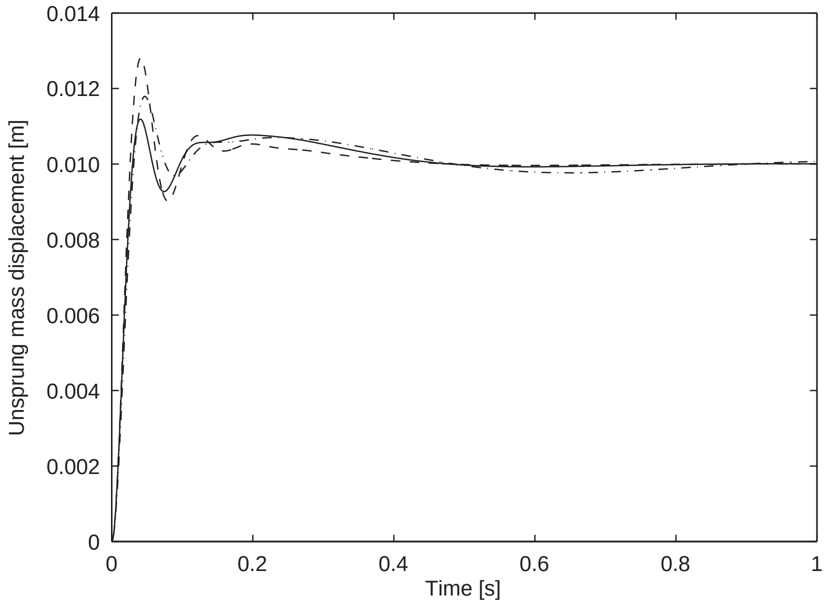

Fig. 8. Unsprung mass displacement versus time: · – ··, passive; – –, LQG; —, A-i-O.

Investigation of Figs. 5–8 shows that, compared with the active suspension based on the LQG, the one based on the A-i-O method is better controlled both in sprung mass acceleration and in unsprung mass displacement with less overshoot, the peak total secondary suspension force or

Table 5
Comparison of the response characteristics for passive and active suspensions

	LQG	Passive	A-i-O	A-i-O1
m_2 displacement overshoot %	8.5	45.3	10.4	8.5
m_1 displacement overshoot %	28.0	18.0	11.9	25.9
Peak total m_2 force (N)	7.3×10^2	8.2×10^2	7.12×10^2	5.75×10^2
Peak actuator force (N)	7.3×10^2	0.0	-2.50×10^2	-4.35×10^2
Peak m_2 acceleration (m/s^2)	2.53	2.83	2.05	1.66
$\int_0^\infty 10^4(x_2 - x_1)^2\,dt$	0.076	0.085	0.073	0.089
$\int_0^\infty 10^5(x_1 - w)^2\,dt$	0.134	0.144	0.129	0.141
$\int_0^\infty 10^4\ddot{x}_2^2\,dt$	1540.1	2145.2	1016.9	721.8
$\int_0^\infty 10^4\rho u^2\,dt$[a]	0.103	0.0	0.021	0.041
$\int_0^\infty 10^4\,\rho(u+f_{pass})^2\,dt$	0.103	0.143	0.098	0.069

[a] $\rho = 8.0 \times 10^{-10}$ [6].

total sprung mass force is less, and the sprung mass displacement is almost the same. Compared with the passive suspension, the performance improvement based on the A-i-O method is greater than that based on the LQG. Both active suspensions are much better controlled than the passive suspension in sprung mass displacement with lower peak sprung mass forces.

The numerical results are listed in Table 5. Results demonstrate that the optimized system based on the A-i-O outruns its counterpart based on LQG in the mean-square values of all aspects, i.e. suspension working space $x_2 - x_1$, dynamic wheel load or $x_1 - w$, sprung mass acceleration $\ddot{x}_2$, actuator force u, and total sprung mass force $u + f_{pass}$. Based on the quadratic performance indices shown in Table 5, the active suspensions based on both the LQG and A-i-O are superior to the passive suspension.

To further investigate the actuator forces based on the A-i-O and LQG, part of Fig. 6 is repeated in Fig. 9. Note that in Fig. 6, the total secondary suspension force based on the A-i-O consists of two sections, the active force (actuator force, denoted as A-i-O (active)) and the passive force (summation of passive spring (k_2) and damper (c_2) forces, denoted as A-i-O (passive)). A close observation of Fig. 9 reveals that, at a point when the road unit input acts on the unsprung mass, the corresponding active suspension force actively resists the disturbance immediately, but the corresponding passive suspension force just follows the disturbance. The resistance to the road disturbance contributes to the performance improvement of the corresponding suspension. Compared with the case of LQG, in the case of A-i-O, the active force resistance to the road disturbance lasts longer and the active force and the corresponding passive force are almost out of phase. This outphase between the active and passive forces in the case of A-i-O makes the corresponding total force smaller than the active force based on the LQG and leads to the performance improvement over the active suspension based on the LQG algorithm. In the case of LQG, although the active force resists the road disturbance, this resistance lasts a very short period of time. Then the active force follows the trends of the passive suspension force based on the A-i-O. Thus, the actuator force based on the A-i-O and that based on the LQG are also almost

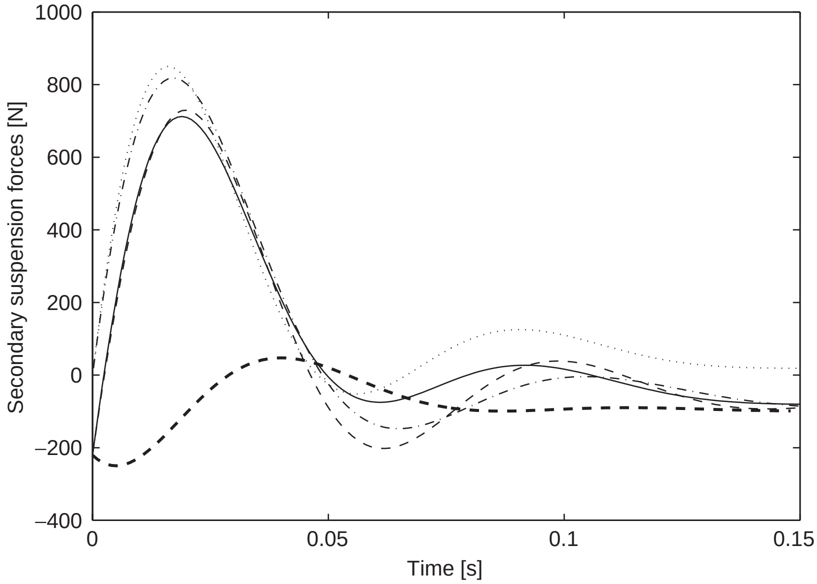

Fig. 9. Secondary suspension forces and their parts versus time: · — ··, passive; - - -, LQG; —, A-i-O (total); **- - -**, A-i-O (active); · · · · ·, A-i-O (passive).

out of phase. This outphase of the actuator force between the two cases can be explained by the opposite sign of $K_{1,3}$ in the control gain matrices for the two cases, as shown in Table 3. Moreover, compared with the case of LQG, in the case of A-i-O, the peak actuator force is much less because of the co-existence of the passive spring and damper.

Notice that the optimized vehicle system based on the A-i-O achieves the above superior performance even though the sprung mass is 20% larger than the mass used in the corresponding vehicle model with the active suspension based on the LQG and the passive suspension.

To examine the effect of the weighting factors or components of objective function shown in Eq. (28) on the performance of the vehicle system, weighting factor ρ_1 takes the value of 7.779×10^{-9} instead of 0.0, the constant v is set to the value of 1.0, and the other weighting factors take the values as those in the case of A-i-O. Note that the weighting factor ρ_1 is determined based on Thompson's [6] quarter-vehicle model with active suspension using the method expressed in Eq. (31) and Thompson did not include the acceleration term in his objective function. To distinguish this case from the previous cases, this case is denoted as A-i-O1. In the case of A-i-O1, the passive vehicle system design variables m_1, m_2, k_1, k_2, and c_2 are also permitted to vary by 20% from the nominal values. We can obtain the optimized passive design variables for this case as listed in Table 4 using the A-i-O method. It can be found that the obtained passive system design variables are the same as those obtained in the A-i-O case except for the minor difference of the variables k_2 and c_2. As a matter of fact, during the numerical experiments using the A-i-O method, the GA does not converge at certain values for the design variables k_2 and c_2 over a narrow value range for both k_2 and c_2 where the performance index J reaches its minimum value. This can be interpreted that within certain value ranges of k_2 and c_2, and with the introduction of the actuator, the vehicle system performance is not sensitive to the passive suspension design variables k_2 and c_2.

In the case of A-i-O1, the obtained control gain matrix **K** and the numerical simulation results are also offered in Tables 3 and 5, respectively. By including the total secondary suspension force as an additional performance index term, from the optimization point of view, we lay more emphasis on reducing the total sprung mass force and sprung mass acceleration. Simulation results match this expectation. As shown in Table 5, compared with the case of A-i-O, the active suspension denoted as A-i-O1 is much better controlled in total sprung mass force, sprung mass acceleration, and sprung mass displacement overshoot. However, the vehicle performance in suspension working space, dynamic wheel load, and actuator force suffers.

The objective function, as provided by Eq. (28), quadratically penalizes large deviations of the state and control vectors from their desired set point values. Numerical experiments show that the selection of the weighting factors for the objective function is important and greatly affects the implementation of the A-i-O method. With each penalized variable normalized by the mean-square value of the corresponding variable of a reference vehicle model (see Eq. (31)), each term of the objective function can be guaranteed to be at the same order of digital value during the optimization and the GA can effectively coordinate the design criteria of ride comfort, suspension working space, dynamic wheel load, and actuator force. From the designer's point of view, this is a meaningful form of objective function because it requires that only an appropriate reference vehicle model be selected.

6.2. *Random road input case*

6.2.1. *Vehicle system optimization*

The vehicle model was optimized with respect to ride comfort, suspension working space, and dynamic wheel load. Hence, the performance index J also takes the form of Eq. (30), where J_1, J_2, J_3 and J_4 are defined in Table 6. The products $\rho_1 J_1$, $\rho_2 J_2$, $\rho_3 J_3$, and $\rho_4 J_4$ are the measures of actuator force, ride comfort, dynamic wheel load, and suspension working space, respectively.

The performance index formulation (30) should be expressed in the standard format as shown in Eq. (1) for the purpose of finding the solution to the optimization problem. With the performance index (30) and governing equation set (24), based on the A-i-O method, the solution to the optimization problem can be obtained.

6.2.2. *Results and discussion*

In this subsection, the simulation results from the A-i-O method are discussed and compared with those reported by Hac [15]. As will be seen, the optimal vehicle model derived from the A-i-O method has better performance than the corresponding model based on the LQG algorithm (used by Hac) in the mean-square values of actuator force, vertical sprung mass acceleration, suspension

Table 6
The definition of the symbols J_1, J_2, J_3 and J_4

J_1	J_2	J_3	J_4
$E[u^2]$	$E[\ddot{x}_2^2]$	$E[(x_1 - w)^2]$	$E[(x_2 - x_1)^2]$

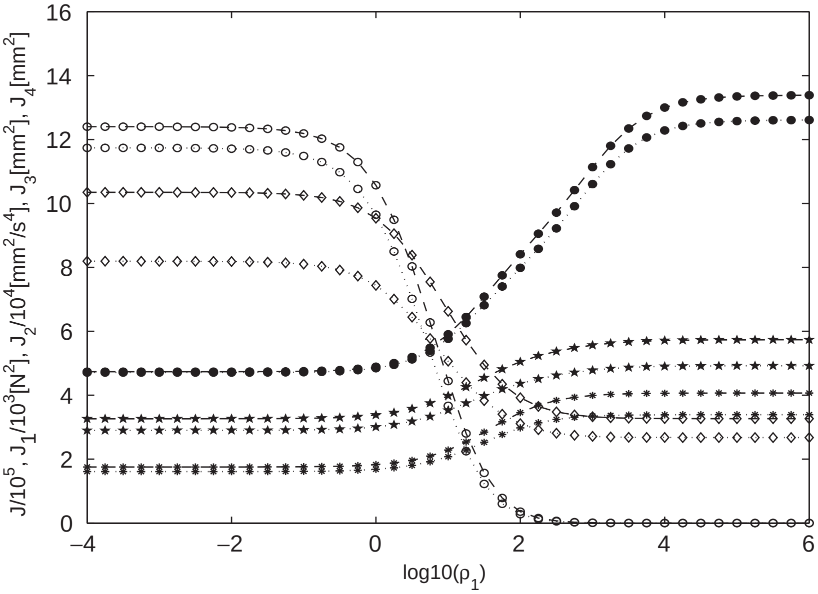

Fig. 10. Performance index J and its parts J_1, J_2, J_3, and J_4 versus ρ_1: —★—, J(LQG); · · ★ · ·, J(A-i-O); —○—, J_1 (LQG); · ·○· ·, J_1 (A-i-O); —◇—, J_2 (LQG); · ·◇· ·, J_2 (A-i-O); —✱—, J_3 (LQG); · ·✱· ·, J_3 (A-i-O); —●—, J_4 (LQG); · ·●· ·, J_4 (A-i-O).

working space, and dynamics wheel load. Note that the simulation results reported by Hac [15] have been accurately repeated in this research.

The vehicle system parameters are listed in Table 1 as Set 2 including the random road characteristic parameters, i.e. a_t and σ_t. When the vehicle is moving at the speed $V = 30\,\text{m/s}$ and the weighting factors $\rho_2 = 1.0$, $\rho_3 = 10^5$ and $\rho_4 = 10^4$, Hac [15] offered the simulation results as shown in Fig. 10. Fig. 10 illustrates the dependence of the performance index (J) and its parts (J_1, J_2, J_3, J_4) upon the weighting factor ρ_1.

The A-i-O method is also used to optimize the vehicle model with passive and active suspension components. The same values used by Hac [15] are assigned to the weighting factors ρ_2, ρ_3, and ρ_4, respectively. However, the vehicle system parameters, i.e. m_1, m_2, k_1, k_2 and c_2 are introduced as additional design variables and these variables are permitted to vary by 10% from the nominal values. Numerical experiments show that the optimized values (denoted as A-i-O) for these design variables are independent of weighting factor ρ_1. The optimal values for these variables are listed in Table 7.

In Fig. 10, the corresponding curves indicate the relationships J, J_1, J_2, J_3, J_4 versus ρ_1 obtained using the A-i-O method. Compared with the optimal suspension based on the LQG, the counterpart based on the A-i-O improves the performance index J and its parts J_1, J_2, J_3, and J_4 over a wide range of weighting factor ρ_1. A close observation shows that, when $\rho_1 < 1$, the latter can achieve much better ride comfort, better road holding capability, and almost the same suspension work space with less actuator force. When $\rho_1 > 10^3$, both suspensions behave like passive suspensions because the actuator force is very small and the latter is superior to the former in ride comfort, suspension work space, and road holding capability.

Table 7
Optimized values for m_1, m_2, k_1, k_2, and c_2

	m_1 (kg)	m_2 (kg)	k_1 (N/m)	k_2 (N/m)	c_2 (N/m/s)
NV[a]	100.0	500.0	2.0×10^5	5.0×10^3	1.0×10^3
A-i-O[b] (±10%)	90.0	550.0	1.8×10^5	5.5×10^3	1.1×10^3
Pass[c] (±10%)	90.0	450.0	1.8×10^5	4.5×10^3	1.1×10^3

[a]Nominal values.
[b]Optimized values based on A-i-O method.
[c]Optimized values for the passive vehicle suspension system using the GA.

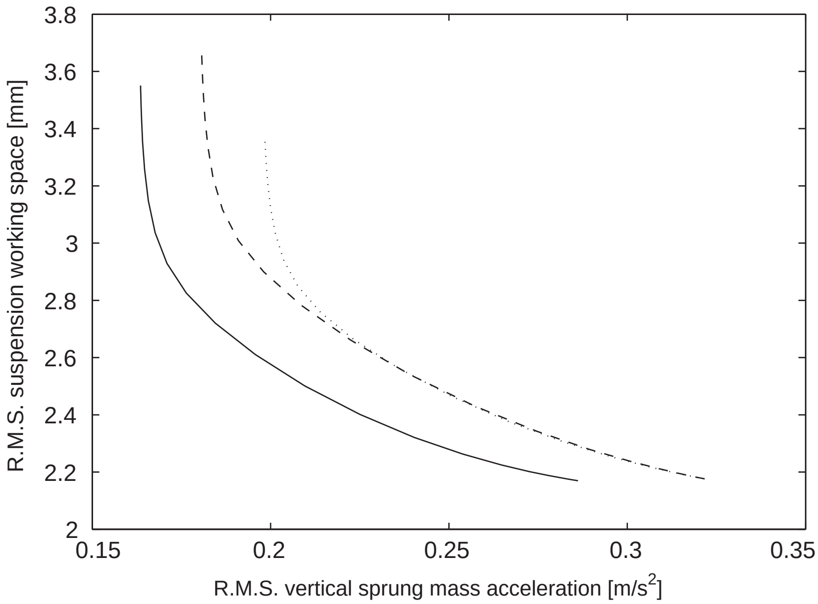

Fig. 11. RMS trade-off solutions of vertical sprung mass acceleration versus suspension working space: – –, LQG; —, A-i-O; · · · · ·, SOP.

To investigate whether a sequential optimization process (SOP), i.e. optimizing the passive vehicle suspension system first, then designing a controller for the system based on the optimized passive vehicle system parameters using the LQG algorithm, can achieve the same results as the A-i-O method does, the GA is used to optimize the passive vehicle suspension system first, then the LQG is applied to the design of the optimal controller for the optimized vehicle system. In these simulations, the weighting factors ρ_2, ρ_3, and ρ_4 are the same as those used with the A-i-O method. The optimized passive vehicle parameters (denoted as Pass) are also listed in Table 7.

Figs. 11 and 12 show the corresponding RMS (root mean square) trade-off solutions of vertical sprung mass acceleration versus suspension working space and RMS trade-off solutions of vertical sprung mass acceleration versus dynamic wheel load for the optimal suspension systems

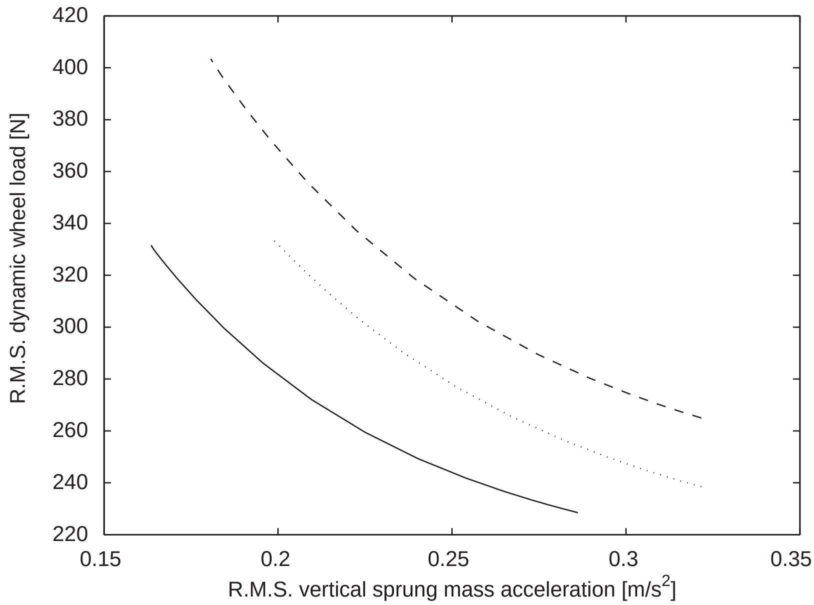

Fig. 12. RMS trade-off solutions of vertical sprung mass acceleration versus dynamic wheel load: – –, LQG; —, A-i-O; · · · · ·, SOP.

based on the A-i-O, the LQG (based on nominal passive vehicle parameter), and the SOP. It is clear that the suspension based on the A-i-O method has the best overall performance among the three optimal suspensions. From Fig. 11, we can see that, within a certain acceleration range, the suspension based on the SOP method requires the largest suspension working space among the three suspensions.

In the simulations, the availability of a limited number of the state variables is considered. As mentioned previously, it is assumed that the absolute vertical velocities of both the sprung mass and unsprung mass (wheel) are available. The simulation results are offered here. In the simulations, the measurement noises are set to 5% of the RMS value of vertical wheel velocity. The simulation results are shown in Fig. 13, which illustrates the dependence of performance indices and measurement errors upon the weighting factor ρ_1. For these simulations, ρ_2, ρ_3, ρ_4, and V still take the values offered previously. In the LQG case (denoted as J_{LQG}), the vehicle system parameters take their nominal values, while in cases of the A-i-O without the Kalman filter (denoted as J_{A1}) and the A-i-O with the Kalman filter (denoted as J_{A2}), the vehicle system parameters are treated as design variables and are permitted to vary by 10% from their nominal values.

As expected, by comparing the results from J_{A1} and J_{A2}, we can see that the performance of the active suspension based on J_{A2} suffers from the measurement corruption. As mentioned previously, when $\rho_1 > 10^3$, the active suspensions behave like passive suspensions. This point can be further demonstrated by the fact that the measurement error J_r becomes very small and the performance indices from J_{A1} and J_{A2} are very close when $\rho_1 > 10^3$. By comparing the results based on J_{LQG} and J_{A2}, we can observe that even though the suspension system based on J_{A2}

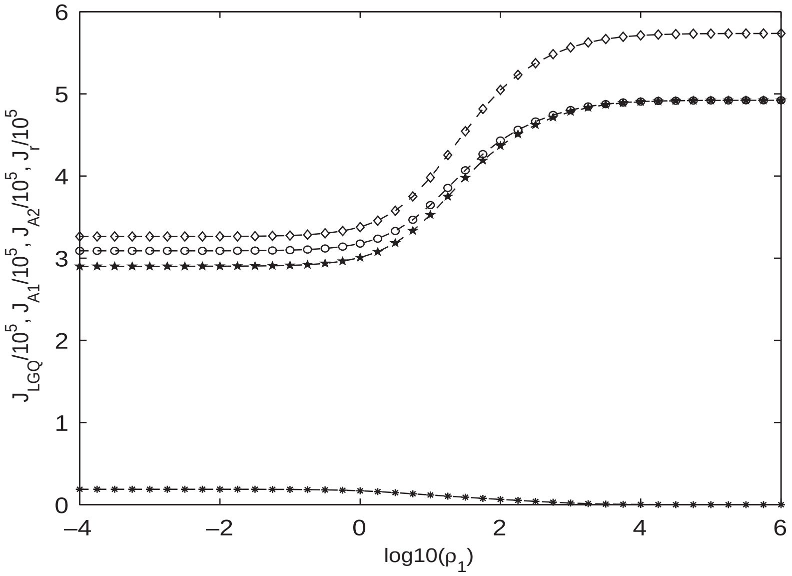

Fig. 13. Performance indices and measurement error J_r versus weighting factor ρ_1: –◇–, J_{LQG} (LQG); –○–, J_{A_2} (A-i-O with Kalman filter); –★–, J_{A_1} (A-i-O without Kalman filter); –✱–, J_r (Measurement errors).

suffers from the measurement errors, its performance is still better than that of the suspension system based on J_{LQG}.

7. Conclusions

This paper demonstrates the feasibility and efficacy of applying a multidisciplinary optimization method, i.e. All-in-One (A-i-O) method, using genetic algorithms, multibody dynamics, the linear quadratic Gaussian method, and the Kalman filter algorithm to the design optimization of mechatronic vehicles with active suspensions. The A-i-O method is implemented in a sophisticated simulation environment in such a way that the linear mechanical vehicle model is designed in the A'GEM program, the optimal controller and Kalman estimator are designed in the MATLAB, then the combined system including mechanical vehicle model, optimal controller, and Kalman estimator is optimized simultaneously by using genetic algorithms.

The A-i-O method is used to resolve the conflicting requirements for ride comfort, suspension work spaces, and dynamic wheel loads in the optimization of quarter-vehicle models with active suspensions. In the simulations, both random and deterministic road inputs and both perfect measurement of full state variables and estimated limited state variable cases are considered. The time domain analysis and covariance analysis are carried out.

Numerical results show that the active suspension systems based on the A-i-O have better overall performance than those derived using the LQG method. The sequential optimization process can not achieve the results obtained by the A-i-O. Based on an appropriately selected reference vehicle dynamic model, by means of normalizing each term of the required objective function, the design optimization using the A-i-O method is greatly facilitated. With the co-existence of passive and active components in vehicle suspensions and the design variables determined by using the A-i-O method, the corresponding actuator forces can actively resist road disturbances much longer than the actuator forces based on the case where the corresponding suspensions have no passive elements and the design variables are determined by using the LQG algorithm.

The above A-i-O method can be applied to the design optimization of complex vehicle models with active suspensions. As a continuation of this research, the application of the A-i-O method to the design optimization of a half vehicle model with flexible vehicle body and active suspensions is under way.

Acknowledgements

Financial support of this research by the Natural Sciences and Engineering Research Council of Canada and by Bombardier Inc. of Canada is gratefully acknowledged. The authors would also like to acknowledge Professor R. Anderson at Queen's University, Canada, for providing the A'GEM software. The authors further acknowledge Professor G. Andrews at the University of Waterloo, for his careful reading of the Ph.D. thesis of the leading author, from which this paper is derived.

References

[1] D. Bestle, Optimization of automotive systems, in: E.J. Haug (Ed.), *Concurrent Engineering: Tools and Technologies for Mechanical System Design*, Springer, Berlin, 1994, pp. 274–296.

[2] W. Schiehlen, Symbolic computations in multibody systems, in: M. Pereira, J. Ambrosio (Eds.), *Computer-Aided Analysis of Rigid and Flexible Mechanical Systems*, 1994, pp. 101–136.

[3] A. Baumal, J.J. McPhee, P. Calamai, Application of genetic algorithms to the optimization of an active vehicle suspension design, *Computational Methods in Applied Mechanical Engineering* 163 (1998) 87–94.

[4] Y. He, J. McPhee, Design optimization of rail vehicles with passive and active suspensions: a combined approach using genetic algorithms and multibody dynamics, *Vehicle System Dynamics* 37 (Suppl.) (2002) 397–408.

[5] D. Karnopp, Design principles for vibration control systems using semi-active dampers, *Journal of Dynamics Systems Measurement Control* 112 (1990) 448–455.

[6] A. Thompson, An active suspension with optimal linear state feedback, *Vehicle System Dynamics* 5 (1976) 187–203.

[7] T. Mei, R. Goodall, LQG and GA solution for active steering of railway vehicles, *IEE Proceedings on Control Theory and Applications* 147 (1) (2000) 111–117.

[8] R. Anderson, The A'GEM multibody dynamics package, *Vehicle System Dynamics* 22 (1993) 41–44.

[9] S. Kodiyalam, J. Sobieski, Multidisciplinary design optimization—some formal methods, framework requirements, and application to vehicle design, *International Journal of Vehicle Design* 25 (1/2) (2001) 3–22.

[10] D. Bestle, P. Eberhard, Dynamic system design via multicriteria optimization, in: G. Fandel, T. Gal (Eds.), *Multiple Criteria Decision Making: Proceedings of the 12th International Conference on Multiple Criteria Decision Making*, Springer, Berlin, 1995, pp. 467–478.

[11] J. Sobieski, R. Haftka, Multidisciplinary aerospace design optimization: survey of recent developments, *Structural Optimization* 14 (1) (1997) 1–23.

[12] J. Sobieski, J. Kodiyalam, R. Yang, Optimization of car body for noise, vibration and harshness and crash, in: *Proceedings of the 41st AIAA/ASME/AHS/ASC, Structures, Structural Dynamics, and Materials*, Number AIAA-2001-1273, Atlanta, 2000.

[13] R. Yang, L. Gu, C. Tho, J. Sobieski, Multidisciplinary design optimization of a full vehicle with high performance computing, in: *Proceedings of the 42nd AIAA/ASME/AHS/ASC, Structures, Structural Dynamics, and Materials*, Number AIAA-2001-1273, Seattle, Washington, 2001.

[14] D. Goldberg, *Genetic Algorithms in Search, optimization, and Machine Learning*, Addison-Wesley, Reading, MA, 1989.

[15] A. Hac, Suspension optimization of a 2-DOF vehicle model using stochastic optimal control technique, *Journal of Sound and Vibration* 100 (3) (1985) 343–357.

[16] A. Bryson, Y. Ho, *Applied Optimal Control, Optimization, Estimation and Control*, Wiley, New York, 1975.

[17] M. Hady, D. Crolla, Active suspension control algorithms for a four-wheel vehicle model, *International Journal of Vehicle Design* 13 (2) (1992) 144–158.

[18] A. Alexandridis, T. Weber, Active vibration isolation of track cabs, *American Control Conference*, San Diego, CA, 1984, pp. 1199–1208.

[19] R. Chalasani, Ride performance potential of active suspension system–Part 2: comprehensive analysis based on a full-car model, in: L. Segel, J. Wong, E. Law, D. Hrovat (Eds.), *Symposium on Simulation and Control of Ground Vehicles and Transportation Systems*, New York, 1986, pp. 205–226.

[20] A. Hac, Stochastic optimal control of vehicles with elastic body and active suspension, *Journal Dynamic Systems Measurement and Control* 108 (1986) 106–110.

[21] J. Hedrick, H. Firouztash, The covariance propagation equation including time-delayed inputs, *IEEE Transactions on Automatic Control* AC-19 (4) (1974) 587–589.

[22] A. Thompson, Optimal and suboptimal linear active suspensions for road vehicles, *Vehicle System Dynamics* 13 (1984) 61–72.